RSC Advances

PAPER

View Article Online
View Journal | View Issue

Cite this: *RSC Adv.*, 2021, **11**, 36089

Formulation of nanopesticide with graphene oxide as the nanocarrier of pyrethroid pesticide and its application in spider mite control†

Xiaoduo Gao,‡[ab] Fengyu Shi,‡[ab] Fei Peng,[cd] Xuejuan Shi,[ab] Caihong Cheng,[cd] Wenlong Hou,[cd] Haicui Xie,[ab] Xiaohu Lin*[c] and Xiuping Wang*[bc]

Nanopesticides with controlled release can achieve more effective utilization of pesticides. Here, to enhance the adsorption of pesticides onto the target organisms, the formulation of pesticides with temperature-responsive release was proposed by combing graphene oxide (GO) and existing pyrethroid pesticides (cyhalothrin, bifenthrin and fenpropathrin). Pesticides were loaded onto GO nanosheets as a carrier *via* a simple physisorption process, and the GO–pesticide nanocomposites exhibited temperature-responsive release and excellent storage stability, which are of vital importance to the practical application. Furthermore, we assessed the bioactivity of the GO–pesticide nanocomposites against spider mites (*Tetranychus urticae* Koch) indoors and in the field. As a result, GO–pesticide nanocomposites had many folds higher bioactivity than individual pesticides, and could be adsorbed on the cuticle of *T. urticae* and surface of bean leaves with highly uniform dispersibility. The easy preparation and higher bioactivity of GO–pesticide nanocomposites indicate their promising application potential in pest control and green agriculture.

Received 29th August 2021
Accepted 24th October 2021

DOI: 10.1039/d1ra06505j

rsc.li/rsc-advances

1. Introduction

Pesticides are widely used to protect crops from diseases, weeds and insects to ensure proper quality control and management in production.[1] However, the toxicity and stability under natural decomposition and persistence in the environment of various pesticides have aroused great public concern.[2,3] As a matter of fact, only a small amount of pesticides can finally reach the targets, while more than 90% of applied commercial pesticides fail to fully exert their bioactivity due to degradation, volatilization and leaching.[4–6] In addition, the low efficiency and overuse of pesticides have also caused many serious problems, such as environmental pollution, adverse health impact and pesticide resistance.[7,8] Therefore, it is urgent to develop alternative agents for improving the efficacy of pesticides and at the same time minimizing their side effects.[9]

Formulation of nanomaterial-based pesticides may improve the efficiency and reduce harmful chemicals to non-target organisms.[10–12] Graphene oxide (GO) is a two-dimensional nanomaterial, and is well-dispersed in water with great adsorption capacity for organics due its hydrogen bonding, π-electron system and large surface area. GO has been intensively investigated as a novel drug delivery agent with a significant synergistic effect on drugs due to several advantages in biomedicine and agricultural science.[13–17] Recently, the application of GO in pesticides for plant protection has attracted great research interests. It has been demonstrated that loading with GO and modification with polydopamine can achieve the controlled release and enhance the leaf surface adsorption properties of hydrophilic pesticides, thereby improving their utilization efficiency.[18] Wang *et al.* have shown that polylactic acid–GO–pesticide has better fungicidal activity against *Rhizoctonia solani* than commercial pyraclostrobin microcapsule suspension.[19] Moreover, the combination of GO with water insoluble pesticides through covalent or non-covalent bonding can synthesize GO–pesticides with a higher pesticide loading rate and better targeted delivery.[20,21] It has been reported GO has multifunctional and synergistic effects with pesticides to enhance the bioactivity against lepidopteran insects.[22] These findings imply that GO may be a promising carrier for pesticides in pesticide formulation.

[a]*College of Agronomy and Biotechnology, Hebei Normal University of Science and Technology, Qinhuangdao 066000, PR China*

[b]*Hebei Key Laboratory of Crop Stress Biology (in preparation), Hebei Normal University of Science and Technology, Qinhuangdao 066000, PR China. E-mail: wangxiuping0721@163.com*

[c]*Analysis and Testing Center, Hebei Normal University of Science and Technology, Qinhuangdao 066000, PR China. E-mail: xiaohulin2008@163.com*

[d]*Hebei Key Laboratory of Active Components and Functions in Natural Products (under planning), Hebei Normal University of Science and Technology, Qinhuangdao, 066004, PR China*

† Electronic supplementary information (ESI) available. See DOI: 10.1039/d1ra06505j

‡ These two authors contributed equally.

Cyhalothrin (Cyh), bifenthrin (Bif) and fenpropathrin (Fen) are three broad-spectrum pesticides and acaricides, which are registered globally for the control of a wide range of pests, and widely used in agricultural production due to their high bioactivities.[23] However, the application of these pesticides is largely hindered by the low utilization efficiency and resultant environmental pollution due to their quick release and unstable properties.[24,25] In the present study, we combined these existing pesticides with GO to formulate new GO–pesticide nanocomposites, and tested their effects on the spider mite (*Tetranychus urticae* Koch), one of the most important phytophagous mite pests for agricultural crops worldwide. This study aims to (1) screen the optimal combined ratio of GO and pesticides, which may determine the bioactivity of the GO–pesticide nanocomposites; (2) characterize the morphology, pesticide loading, release behavior and storage stability of GO–pesticide nanocomposites; and (3) determine the bioactivity of the GO–pesticide nanocomposites against the spider mites in the indoor and field. The findings may provide important implications for the development of new formulations of nanopesticides.

2. Materials and methods

2.1. Materials

All chemicals were of analytical grade and used as received without further purification. Graphite was purchased from Qingdao Tianhe Graphite Co. Ltd., with an average particle diameter of 4 mm (99.95% purity). All other reagents were of high performance liquid chromatography (HPLC) grade, and obtained from the Tianjin No. 3 Chemical Plant. Cyh, Bif and Fen (ACS grade) were purchased from Sigma-Aldrich.

2.2. Spider mites and rearing

Colonies of *T. urticae* were obtained from a research colony maintained on bean (*Phaseolus vulgaris* L.) plants without any pesticide exposure. *T. urticae* was maintained in a growth chamber at 25 ± 2 °C, 60 ± 5% relative humidity, and 14 : 10 h light: dark photoperiod.[26]

2.3. Preparation of GO–pesticide nanocomposites

Commercially available graphite powder was oxidized and exfoliated to GO by a modified Hummers' method.[27] GO–pesticide nanocomposites were prepared by physical loading of pesticides onto the surface of GO.[20] Briefly, the pesticides of different mass were dispersed in 2 mL mixture of dichloromethane, Tween 20 and water solution (DT, 1 : 1: 98, v/v). Then, GO was added to make the final mass ratio of pesticide and GO to be 1 : 9, 2 : 8, 3 : 7, 4 : 6, 5 : 5, 6 : 4, 7 : 3, 8 : 2 and 9 : 1. The mixture was then stirred in dark for 24 h. The obtained product was washed with deionized water and freeze-dried for further use. The morphology of GO and GO–pesticide nanocomposites was examined by scanning electron microscopy (SEM, Hitachi, SU8010). Infrared absorption spectra of GO and GO–pesticide nanocomposites were measured on a Fourier transform infrared (FT-IR) spectroscope (Bruker, TENSOR-27) at room temperature. Thermogravimetric analysis (TGA) was performed with a STA 409 PC (Netzsch, Germany) from room temperature to 700 °C at a heating rate of 10 °C min^{-1} under N_2 atmosphere. GO–pesticide was dropped on the paraffin film, and the contact angle was recorded by contact angle measurement (Dataphysics, OCA20, Germany).

2.4. Determination of the pesticide-loading capacity of GO

The loading amount of pesticides on the surface of GO was measured by HPLC. HPLC (Dionex U3000, USA) was employed by using ZORBAX Eclipse Plus C_{18} column (250 mm × 4.6 mm, 5 μm; Agilent, USA) with UV detection at 278 nm (Cyh and Fen) or 238 nm (Bif). A flow rate of 1 mL min^{-1} was used with a mobile phase composition of methanol and water (90 : 10, v/v), and the injection volume was 10 μL. For determination of the loading amount, the prepared GO–pesticide nanocomposites were dissolved in deionized water. The pesticide loading content (LC) was obtained with the following equation:[28]

$$\mathrm{LC}\ (\%) = W_{\mathrm{pesticide}}/W_{\mathrm{GO}} \times 100,$$

where $W_{\mathrm{pesticide}}$ is the weight of pesticide loaded on GO (μg), and W_{GO} is the weight of GO (μg).

2.5. *In vitro* release experiment

A dialysis method was used to evaluate the release behavior of pesticides from GO–pesticide nanocomposites.[29] Briefly, 5 mL of GO–pesticide nanocomposite dispersion was added to a dialysis bag with a molecular weight cutoff of 3500 Da (Mym Biological Technology Co., Ltd). Then, the dialysis bag was immersed in 45 mL of methanol–water mixture (6 : 4, v/v) in a centrifuge tube. All centrifuge tubes were shaken at a speed of 200 rpm at 25 °C and 35 °C. About 1 mL of supernatant was sampled at different intervals, with the addition of 1 mL fresh medium each time. The sample solution was filtered through a cellulose-membrane filter (diameter, 13 mm; pore size, 0.22 μm; Dikma Technologies Inc.) and then injected into the HPLC system to measure the concentration of pesticides. The release kinetics was calculated with the empirical equation proposed by Ritger and Peppas.[30]

$$M_t/M_z = kt^n,$$

where M_t/M_z is the percentage of pesticide release at time t. k is the constant that incorporates the characteristics of the GO–pesticide nanocomposite system and the pesticide, and n is the diffusion parameter indicative of the transport mechanism. The time taken for the release of half pesticide into the medium (T_{50}) was calculated for the comparison of GO–pesticide nanocomposites and pesticides.

2.6. Storage stability of GO–pesticide nanocomposites

GO–pesticide nanocomposite solutions (containing 1 mg mL^{-1} pesticide) were added into glass bottles and kept at 0 °C for 7 d or 54 °C for 14 d. Then, the content of the pesticide was determined by HPLC.[10]

GO–pesticide nanocomposite solution in a glass bottle was placed in a dark, dry and ventilated place for 24 months, and the content of the pesticide was measured every four months by HPLC.[20]

2.7. Bioassay of the acaricidal activity of GO–pesticide nanocomposites in the indoor

The acaricidal activities of GO–pesticide nanocomposites against *T. urticae* were evaluated using leaf dip assays recommended by Spray tower and Petri dish methods.[31,32] The pesticides (Cyh, Bif and Fen) in individual or combined with GO were used to treat *T. urticae* as described in Table 1. Adult *T. urticae* females were transferred from the source culture with the *T. urticae* infested leaves to fresh bean leaves. Forty adult females were placed on every fresh leaf placed on a wet filter paper in a Petri dish (9 cm diameter) and surrounded with Vaseline to prevent the escape of mites. After 2 h, the dead and inactive individuals were removed using an insect needle under a stereo microscope (Zeiss, Stemi 305). The pesticide suspensions described in Table 1 were sprayed on the leaf containing mites by a Potter spray tower (Auto-Load; Burcard® Scientific) at one bar pressure (2 μL cm^{-1} 2 suspension). An equal volume of DT solution without any pesticides was processed similarly to the control (negative control). The treated *T. urticae* was kept in an incubator at 25 ± 1 °C, 60 ± 5% RH and L16 : D8 h photoperiod. After 24 h, a small brush was used to touch the body of *T. urticae* to evaluate its viability under a stereo microscope. Individuals without any movement of appendages were recorded as dead. The criterion of the test for effectiveness was that the mortality of the control treatment was less than 10%.

2.8. Acaricidal activities of GO–pesticide nanocomposites in greenhouse

Greenhouse bioassays were performed to determine the acaricidal activities of Cyh, Bif and Fen in individual or combined with GO using greenhouse-grown bean as the host plant. The suspensions described in Table 1 (5 mL for each plant) were uniformly sprayed with a hand sprayer (JB-11 trigger sprayer, 250 mL, Taizhou Qiyong Agricultural Machinery Co., Ltd, Taizhou, China) onto the surface of plant leaves. Each of the five plants in each plot was sprayed with 5 mL DT as the negative control. The number of dead mites was recorded 7 days after treatment. Each treatment was replicated thrice.

Table 1 Bioassays of Cyh, Bif and Fen in individual or combined with GO against *T. urticae*

	Concentrations of test (μg mL^{-1})	
Treatment	Indoor	Greenhouse/Field
DT	Dichloromethane, Tween 20 and water solution (1 : 1 : 98, v/v)	
Cyh/Bif/Fen	62.5, 125, 250, 500	125, 250, 500, 1000
GO–Cyh	37.5, 75, 150, 300	75, 150, 300, 600
GO–Bif/Fen	31.25, 62.5, 125, 250	62.5, 125, 250, 500

2.9. Acaricidal activities of GO–pesticide nanocomposites in field

The assay of acaricidal activity in the field was performed according to "the Chinese National Standard Guidelines for Field Efficacy Trials: Acaricides Against Mites in Beans and Vegetables" (GB/T17980.17-2000). Field trials were carried out in the Experimental Station of Hebei Normal University of Science and Technology in July 2021. As shown in Table 1, Cyh, Bif and Fen in individual or combined with GO were tested against *T. urticae* on bean plants. DT solution was used as the control. A randomized complete block design consisting of three replicates of 25 treatments (75 plots) was adopted for each study site, with random assignment of treatments to plots within each block. Each plot was 20 m^2 in area, and a protective barrier consisting of four rows of eggplant was set up around the test field. A individual treatment was performed in each field test, and the total spray volume was 750 L ha^{-1} using a 3WJD-18 knapsack electric sprayer (pressure of 0.4 MPa) (Shandong Weishi Plant Protection Machinery Co., Ltd.), with a nozzle hole diameter of 1 mm.[33] The number of total mites was recorded before the treatment and that of dead mites was recorded after 7 days of treatment.

2.10. Observation of changes in the morphology of spider mites

In order to better explore the effect of GO incorporation to enhance the acaricidal activity of pesticides, we examined how GO and GO–pesticide nanocomposites interacted with spider mites by SEM imaging. The spider mites were treated with DT, GO, Cyh, GO–Cyh, Bif, GO–Bif, Fen and GO–Fen, respectively, as described above. Then, 10 individual spider mites were fixed with 2.5% glutaraldehyde using a vacuum pump in an ice bath for 30 min, followed by 4 h of incubation at 4 °C and three times of washing with PBS. Subsequently, the spider mites were dehydrated through an ethanol series and examined under a SEM.[34]

2.11. Statistical analysis

Abbott's formula was used to correct the mortality data.[35] All data presented in the tables were expressed as the mean ± SE of triplicate measurements. The corrected mortality was normalized by arcsine square-root transformation before one-way analysis of variance (ANOVA) followed by a least significant difference (LSD) test at $P < 0.05$ using SAS Institute (2002; SAS Institute, Cary, NC). The mortality data were analyzed by probit analysis to determine the median lethal concentration (LC_{50}) and 95% confidence limit (CL).[36] χ^2 value was used to measure the goodness-of-fit of the probit regression equation. To assess the degree of synergism, the synergistic ratio (SR) was calculated by dividing the LC_{50} of the individual pesticide by that of nano-pesticide. The SR values between 0.5 and 1.5 represent additive interactions; and those higher than 1.5 indicate synergistic interactions.[33]

3. Results and discussion

3.1. Screening of the optimal ratio of GO and pesticides

In order to screen the optimal combination ratio of GO with three pesticides, the mortality of *T. urticae* treated by GO–

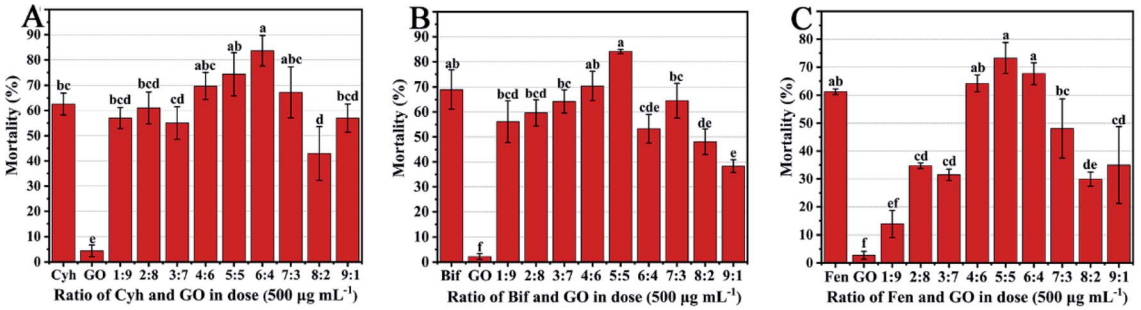

Fig. 1 Mortality of *T. urticae* treated by individual pesticides or combined with GO at different mass ratios. Mortality of *T. urticae* treated by Cyh and GO (A), Bif and GO (B), Fen and GO (C) at different mass ratios. Data are mean ± stand error (SE). Error bars represent the SE ($N = 3$). Different lowercase letters indicate significant differences between treatments ($p < 0.05$).

pesticide nanocomposites at different mass ratios was tested. As shown in Fig. 1A, the mortality of *T. urticae* under treatments of individual Cyh and GO was 62.57% and 4.45%, respectively, while reached 83.65% under treatment with GO–Cyh combined at a mass ratio of 6 : 4, which was screened as the optimal combination ratio of Cyh and GO. GO–Bif combined at the ratio of 5 : 5 showed higher acaricidal activities than other combinations (Fig. 1B), and GO–Fen combined at the ratios of 5 : 5 and 6 : 4 resulted in the highest mortality (Fig. 1C). Considering the cost and feasibility in practical application, we chose GO–Cyh, GO–Bif and GO–Fen combined at 6 : 4, 5 : 5 and 5 : 5 as the optimal combinations for subsequent characterization and bioassay analysis.

3.2. Morphology of formulated GO–pesticide nanocomposites characterized by SEM

In order to explore the structural characteristics, the morphology of GO, individual pesticides and GO–pesticide nanocomposites was determined by SEM. GO exhibited typical wrinkles as shown in Fig. 2A,[37] while the three pesticides were crystal with rectangular parallelepiped structure, smooth surface and different size (Fig. 2A–C). After loading of pesticides, large amount crystals with rectangular parallelepiped structure were observed on GO surface (Fig. 2D–F), indicating that the appearance of these crystals was due to the adsorption of Cyh, Bif and Fen on GO sheets, which would be further verified by FT-IR later.

3.3. FT-IR characterization of GO–pesticide nanocomposites

The spectra of GO show the characteristic peaks including O–H stretching at 3415 cm^{-1}, skeletal vibration of graphitic domains at 1726 cm^{-1} and 1620 cm^{-1}, C–OH stretching at 1362 cm^{-1}, and C–O stretching at 1076 cm^{-1}.[38–40] In the spectra of Cyh (Fig. 3A), the stretching vibration of the benzene skeleton was at 1585 and 1487 cm^{-1}, and the carbonyl stretching vibration of ester group appeared at 1724 cm^{-1}.[41] The spectra of GO–Cyh

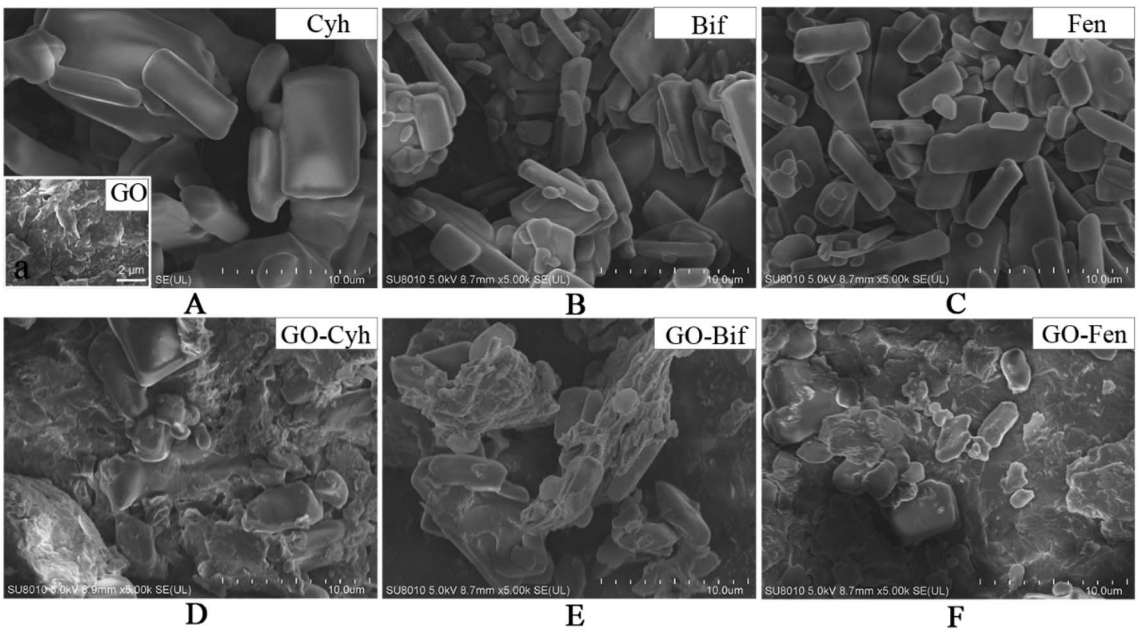

Fig. 2 Morphology characterization of the formulated GO–pesticide nanocomposites. SEM image of GO (Aa), Cyh (A), Bif (B), Fen (C), GO–Cyh at 6 : 4 (D), GO–Bif at 5 : 5 (E) and GO–Fen at 5 : 5 (F).

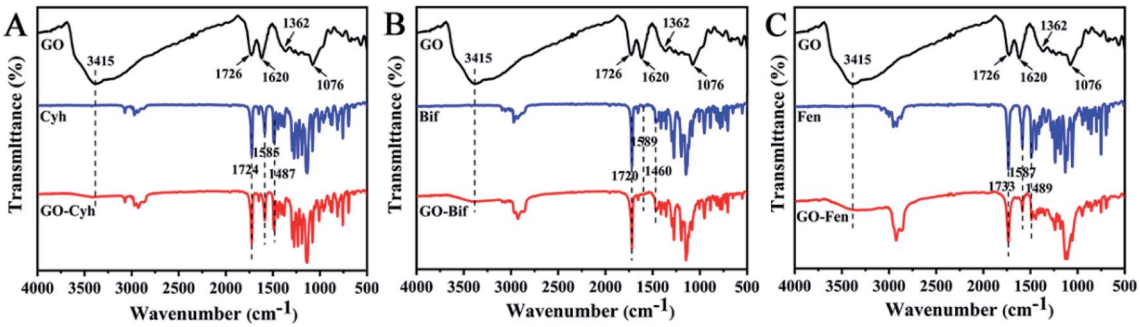

Fig. 3 FT-IR spectra of GO–Cyh (A), GO–Bif (B) and GO–Fen (C).

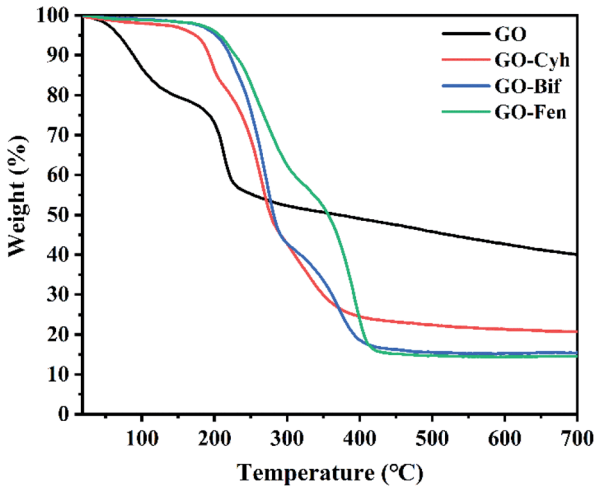

Fig. 4 TGA curves of GO and GO–pesticide nanocomposites.

obviously include the characteristic peaks of both GO and Cyh without any new peaks (Fig. 3A), indicating that Cyh was physically loaded onto GO without any change in its chemical properties. Similar results were obtained for GO–Bif (Fig. 3B) and GO–Fen (Fig. 3C). These results indicated that the pesticides were loaded onto the surface of GO through physical adsorption.

3.4. Thermal stability analysis of GO–pesticide nanocomposites

Thermal stability analysis was carried out by comparing the TGA curves of GO and GO–pesticide nanocomposites, and the results are shown in Fig. 4. GO showed a weight loss of 27% at 200 °C, while GO–Cyh, GO–Bif and GO–Fen nanocomposites were stable with a weight loss of only about 5%, showing improvement of thermal stability in GO–pesticide nanocomposites.

3.5. Loading performance of GO–pesticide nanocomposites

The loading capacity of pesticides on GO was determined using the HPLC method. The standard curves were obtained for three pesticides at concentrations ranging from 62.5 to 1000 μg mL^{-1}, and the correlation coefficient was higher than 0.999 (Fig. S1†). Then, the loading content of pesticides on GO was calculated. The results showed that the LC of Cyh, Bif and Fen on GO was 122.10%, 77.13% and 74.03%, respectively.

3.6. Release behaviors of GO–pesticide nanocomposites

In order to study their temperature-responsive release behaviors *in vitro*, individual pesticides and GO–pesticide nanocomposites were placed in methanol–water mixture (6 : 4, v/v) at different temperature for a week. At different time points, the supernatant was collected to measure the cumulative release amount by HPLC. The release behaviors of individual pesticides and GO–pesticide nanocomposites are shown in Fig. 5. At the temperature of 35 °C, Cyh was released into the

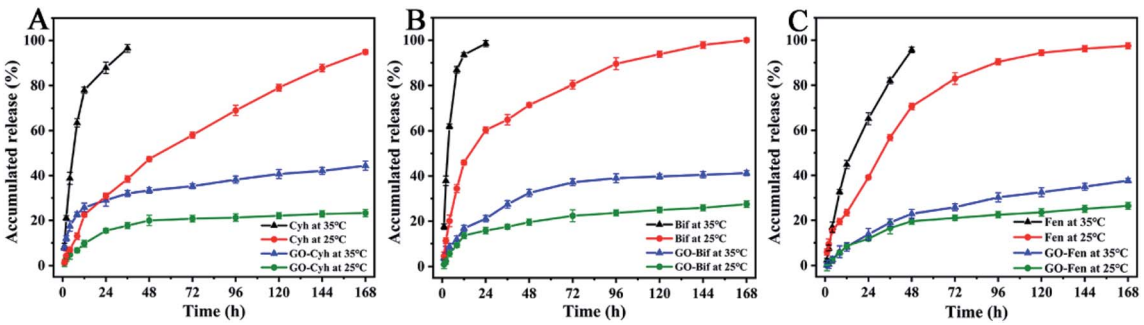

Fig. 5 Release behaviors of individual pesticides and GO–pesticide nanocomposites. Release behaviors of Cyh and GO–Cyh (A), Bif and GO–Bif (B), Fen and GO–Fen (C) at 25 °C and 35 °C. Data are mean ± SE. Error bars represent the SE ($N = 3$).

medium solution at a fast rate, and completely released in 36 h; in contrast, GO–Cyh exhibited excellent sustained-release performance of Cyh, and Cyh release could still be observed after 168 h. In the first 2 h, the release of Cyh from GO–Cyh was relatively fast with a cumulative release rate of 11.99%; after that, the release became fairly slow, and the cumulative release rate was 44.38% after 168 h, which is in conformity with the characteristic release pattern of controlled drug delivery systems. At 25 °C, the cumulative release rate of individual Cyh was 94.90% in 168 h, while that of GO–Cyh was only 23.28% (Fig. 5A). Similar results were obtained for GO–Bif (Fig. 5B) and GO–Fen (Fig. 5C). The initial burst release and subsequent slow release are conducive to the long-term maintenance of effective concentration, which can help to maintain a high activity of the pesticide.[42]

Table 2 presents the release kinetics calculated according to the generalized model $M_t/M_z = kt^n$. The results showed that the pesticide release profile from GO–pesticide nanocomposites had a high correlation with the empirical equation, indicating that the GO–pesticide nanocomposites have a desirable sustained release property.

3.7. Storage stability of GO–pesticide nanocomposites

Long-term storage stability and low- and high-temperature stability of pesticides are very important indices for pesticide formulation, which can guarantee the effective application in agricultural production.[10] Therefore, we evaluated the storage stability of GO–pesticide nanocomposites by measuring the content of effective pesticide components during two years of storage and under low- and high-temperature storage. As shown in Fig. 6A, the contents of pesticides showed no significant loss after low- and high-temperature storage. Besides, the change of the content of pesticides is nearly negligible in the long-term storage after two years of storage (Fig. 6B). Fig. S2† shows the corresponding images of GO–pesticide nanocomposites after low- and high-temperature storage. All of the samples stayed stable with no precipitation or stratification during storage under different temperature (low and high), which visually confirms that the GO–pesticide nanocomposites have stability. Moreover, after two years of storage, the GO–pesticide nanocomposite showed slight precipitation, but could still be evenly dispersed after shaking, which meet the requirements of practical production and application (Fig. S3†).

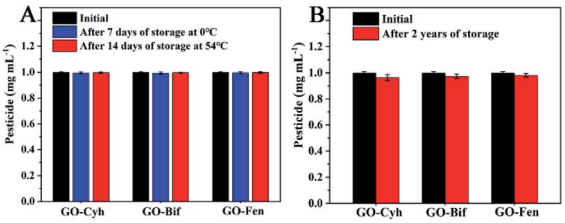

Fig. 6 Low- and high-temperature storage stability of GO–pesticide nanocomposites (A); long-term storage stability (B).

Table 3 Acaricidal activities of individual pesticides and GO–pesticide nanocomposites against *T. urticae* in the indoor at 24 h

Treatment	Slope ± SE[a]	χ^{2b}	P	LC_{50} (95% CL)[c]	SR[d]
Cyh	3.07 ± 0.73	0.36	0.17	9.79 (7.62–11.37)	—
GO–Cyh	1.77 ± 1.49	0.71	0.30	1.93 (1.69–2.07)	5.07
Bif	2.62 ± 0.97	0.11	0.05	11.67 (9.93–14.50)	—
GO–Bif	2.84 ± 1.10	0.24	0.12	2.17 (2.07–2.26)	5.38
Fen	2.87 ± 0.87	0.36	0.16	10.94 (8.65–13.10)	—
GO–Fen	2.61 ± 1.25	0.40	0.06	1.89 (1.74–1.97)	5.79

[a] Slope of the probit mortality line. [b] Goodness-of-fit test. [c] LC_{50} value and 95% confidence limit (CL). [d] Synergism ratio at LC_{50} values.

3.8. Acaricidal activities of GO–pesticide nanocomposites in the indoor

To assess the synergistic effects of GO on pesticides, bioassays were carried out to determine the LC_{50} values of individual pesticides and GO–pesticide nanocomposites against *T. urticae* (Table 3). As a result, Cyh showed a LC_{50} value of 9.79 μg mL^{-1}, while that of GO–Cyh was 1.93 μg mL^{-1} with a SR value of 5.07, indicating that the GO–Cyh nanocomposite was 5.07-fold potent relative to Cyh. The LC_{50} of Bif and Fen was 11.67 μg mL^{-1} and 10.94 μg mL^{-1}, while that of GO–Bif and GO–Fen was

Table 2 Constants from fitting the generalized model, $M_t/M_z = kt^n$, to the release data of pesticides from nanocomposites at 25 °C and 35 °C

Conditions		Diffusion parameter (n)	Release constant (k)	R^2	Half time (T_{50}, hour)
25 °C	Cyh	0.59	4.60	0.99	55.98
	GO–Cyh	0.35	4.20	0.92	1116.18
	Bif	0.35	17.79	0.96	19.98
	GO–Bif	0.36	4.55	0.96	800.59
	Fen	0.48	9.13	0.96	34.16
	GO–Fen	0.47	2.57	0.95	549.74
35 °C	Cyh	0.47	19.93	0.87	7.05
	GO–Cyh	0.28	10.97	0.96	233.56
	Bif	0.38	34.00	0.83	2.79
	GO–Bif	0.37	6.72	0.96	232.93
	Fen	0.68	7.13	0.99	17.72
	GO–Fen	0.56	2.20	0.98	264.11

Table 4 Acaricidal activities of individual pesticides and GO–pesticide nanocomposites against *T. urticae* in greenhouse and in the field

Treatment	Slope ± SE[a]	χ^{2b}	*P*	LC_{50} (95% CL)[c]	SR[d]
Cyh[e]	1.81 ± 1.24	0.90	0.37	57.68 (45.04–69.41)	—
GO–Cyh[e]	2.20 ± 1.18	1.10	0.43	20.60 (15.30–28.90)	2.80
Bif[e]	2.66 ± 0.94	0.56	0.24	97.79 (90.60–105.55)	—
GO–Bif[e]	2.72 ± 1.05	0.06	0.03	27.54 (15.44–39.37)	3.55
Fen[e]	0.76 ± 1.72	0.58	0.34	47.21 (38.05–51.20)	—
GO–Fen[e]	1.28 ± 1.66	0.41	0.19	15.48 (11.42–20.56)	2.85
Cyh[f]	4.41 ± 0.28	0.61	0.26	130.19 (92.58–183.11)	—
GO–Cyh[f]	4.17 ± 0.49	0.59	0.16	48.80 (26.29–90.61)	2.67
Bif[f]	4.41 ± 0.26	0.06	0.03	197.17 (184.36–210.88)	—
GO–Bif[f]	3.34 ± 0.93	0.77	0.33	62.44 (41.01–95.08)	3.16
Fen[f]	4.12 ± 0.47	0.32	0.15	76.84 (38.47–153.48)	—
GO–Fen[f]	4.56 ± 0.43	0.10	0.05	30.56 (16.79–76.40)	2.51

[a] Slope of the probit mortality line. [b] Goodness-of-fit test. [c] LC_{50} value and 95% confidence limit (CL). [d] Synergism ratio at LC_{50} values. [e] Data in the greenhouse. [f] Data in the field.

2.17 μg mL^{-1} and 1.89 μg mL^{-1}, respectively, indicating that the LC_{50} value was significantly decreased by the supplementation of GO. The SR values of GO–Bif and GO–Fen were 5.38 and 5.79, indicating 5.38-fold and 5.79-fold acaricidal activity relative to that of Bif and Fen, respectively. These results suggest that GO has a superior synergistic effect to promote the toxicity of Cyh, Bif and Fen against *T. urticae*.

3.9. Acaricidal activities of GO–pesticide nanocomposites in greenhouse and in the field

Table 4 shows the LC_{50} values of individual pesticides and GO–pesticide nanocomposites against *T. urticae* in the greenhouse and in the field. The results also demonstrated that GO can contribute to a significant synergistic acaricidal activity against *T. urticae*.

In this study, GO–pesticides exhibited better bioactivity than individual pesticides in both indoor and field. We speculate that the enhanced bioactivity after GO incorporation may be ascribed to the context of GO–pesticide composites, which can enhance the effects of pesticides by improving the dispersibility so as to increase the contact between the pesticide and spider mites. GO is well-dispersed in water, but pesticides are generally not dispersible in water. The adsorption of pesticide on GO at the optimal ratio improves the water dispersibility of the pesticide. In addition, dispersibility may strongly affect the interactions of materials with organisms.[43] More dispersible materials, such as GO–pesticides, may have higher bioactivity than those with lower dispersibility (such as Cyh, Bif and Fen), possibly because the pesticides have more opportunities to interact with the spider mites.

3.10. Adsorption of GO–pesticide nanocomposites on the cuticle surface of mites and bean leaves

Fig. 7 shows the typical SEM images of interactions between *T. urticae* and GO, individual pesticides and GO–pesticide nanocomposites after 24 h of treatment. Compared with Fig. 7A, Fig. 7E only shows the adsorption of a large amount of GO on the mites. In contrast to Fig. 7B–D, Fig. 7F–H also show the adhesion of a large amount of GO on mite cuticle. These results reveal that GO can be firmly adsorbed on the cuticle surface of spider mites, though plenty of GO might have been washed off from the cuticle of mites during the slicing process required for SEM analysis.

Moreover, the contact angle was used to evaluate the wettability and adhesion ability of GO–formulation.[21] As shown in Fig. S4,† the contact angles of water, GO–Cyh, GO–Bif and GO–Fen on the surface of paraffin film are about 109.7°, 76.4°, 79.3° and 76.5°, respectively. The GO–pesticide showed a lower contact angle than water, indicating that it has good adhesion ability and spreadability. Fig. S5† shows that GO–pesticide nanocomposites can be adsorbed on the leaves of bean plants with a highly uniform dispersibility, which is very conducive to actual application.

It has been reported that the adsorption of proteins and lipids on GO occurs spontaneously and rapidly through electrostatic, hydrophobic, hydrogen bonding and π–π stacking

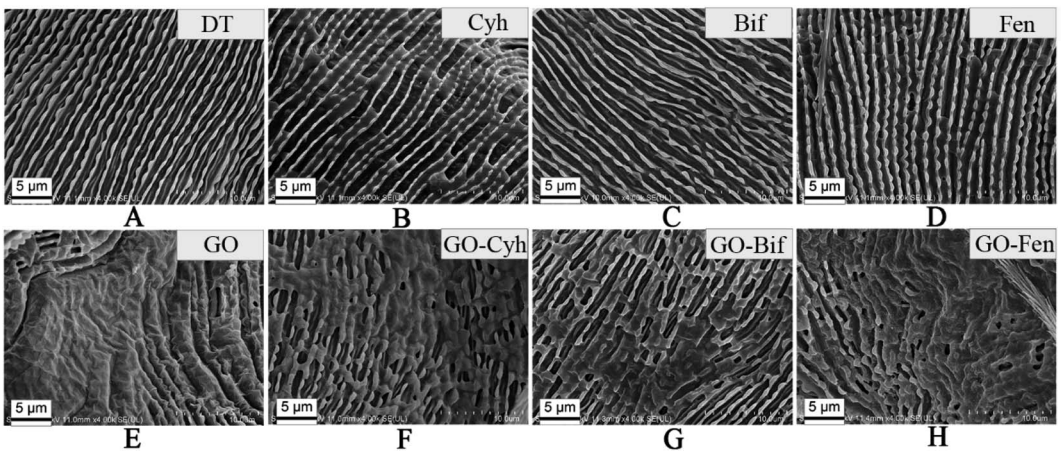

Fig. 7 SEM images of the interactions between *T. urticae* and GO, individual pesticides and GO–pesticide nanocomposites after treatment for 24 h. (A–D) Images of *T. urticae* treated by DT, Cyh, Bif and Fen, respectively. (E–H) Images of *T. urticae* treated by GO and GO–Cyh, GO–Bif and GO–Fen, respectively.

interactions.[44–46] In general, proteins and lipids are the main structural components of mite cuticle.[47] The vast surfaces of plant leaves are protected by a coating of cuticular wax against various abiotic and biotic stresses.[48] Leaf surface wax is a complex mixture of lipid derivatives and triterpenoids as the two major compounds. Thus, we speculate that the adsorption of GO on the cuticle of spider mites and bean leaves is not only due to the deposition of GO–pesticide nanocomposites during impregnation, but also due to the spontaneous interaction of the surface structure of mites and leaves with GO. It can be concluded that GO may be a promising carrier for the delivery of pesticides to spider mites and plant leaves, which may greatly enhance the bioactivities of pesticides.

Moreover, in the formulation process of pesticides, most of active ingredients in the pesticides are hydrophobic compounds, which can be processed into pesticides only under the assistance of organic solvents.[21] The application of large amounts of organic solvents for the dissolution of hydrophobic active ingredients in pesticide formulation may significantly increase the pollution of pesticides to the environment and toxicity to non-target organisms. GO is composed of a single-atom-thick lattice of honeycomb-like sp^2 bonded carbon atoms, including abundant oxygen-containing polar functionalities, such as carbonyl, epoxide, carboxyl and hydroxyl groups.[49] Due to the abundant oxygen functionalities, GO can be easily dispersed in organic solvents, water and different matrices.[50] Therefore, GO can be applied as a water-solubilizing agent for pesticide formulation to reduce the use of organic solvent for lower risks to the environment.

4. Conclusions

In this study, we demonstrate that GO–pesticide nanocomposites have good sustained release, excellent stability under different conditions, and high loading efficiency of pesticides. The pesticides can be adsorbed on the surface of GO through physical adsorption. Besides, the bioactivity of GO–pesticide nanocomposites against *T. urticae* is remarkably higher than that of individual pesticides in the indoor and field. The GO–pesticide nanocomposites can be well adsorbed on the cuticle of spider mites and bean plant leaves with a uniform dispersibility. Therefore, it is feasible to develop intelligent temperature-responsive pesticides for agricultural pest control, which may improve pesticide efficacy and reduce pesticide dosage, and has a promising practical application prospect.

Author contributions

Xiaoduo Gao: methodology, investigation, visualization, writing – original draft; Fengyu Shi: conceptualization, formal analysis, data curation; Fei Peng: formal analysis, resources, supervision; Xuejuan Shi: investigation, methodology; Caihong Cheng: resources, project administration; Wenlong Hou: resources, supervision; Haicui Xie: software; Xiaohu Lin: resources; Xiuping Wang: conceptualization, supervision, funding acquisition, writing – review & editing.

Conflicts of interest

The authors declare no conflict of interest.

Acknowledgements

This research was funded by National Natural Science Foundation of China (31501680), Key Research and Development Program of Hebei Province (21326507D), Modern Agricultural Industrial Technology System Innovation Team of Hebei Province (coarse grains and beans, HBCT2018070404), Science and Technology Research Project for Colleges and Universities in Hebei Province (BJ2020049), Postgraduate Innovation Funding Project of Hebei Province (CXZZSS2020120) and Postgraduate Innovation Funding Project of Hebei Normal University of Science and Technology (CXZZ202103).

Notes and references

1 Y. Abdel-Halim, *Life Sci.*, 2019, **5**, 81–86.
2 A. Singh, N. Dhiman, A. K. Kar, D. Singh, M. P. Purohit, D. Ghosh and S. Patnaik, *J. Hazard. Mater.*, 2020, **385**, 121525.
3 M. I. Swasy, B. R. Brummel, C. Narangoda, M. F. Attia, J. M. Hawk, F. Alexis and D. C. Whitehead, *RSC Adv.*, 2020, **10**, 44312.
4 L. D. Cao, H. R. Zhang, C. Cao, J. K. Zhang, F. M. Li and Q. L. Huang, *Nanomaterials*, 2016, **6**, 126.
5 H. Qin, H. Zhang, L. X. Li, X. T. Zhou, J. P. Li and C. Y. Kan, *RSC Adv.*, 2017, **7**, 52684–52693.
6 G. Asgari, A. Seidmohammadi, A. Esrafili, J. Faradmal, M. N. Sepehr and M. Jafarinia, *RSC Adv.*, 2020, **10**, 7718–7731.
7 A. Singh, N. Dhiman, A. K. Kar, D. Singh, M. P. Purohit, D. Ghosh and S. Patnaik, *J. Hazard. Mater.*, 2020, **385**, 121525.
8 N. N. Lv, K. S. Ma, R. Li, P. Z. Liang, P. Liang and X. W. Gao, *Ecotoxicol. Environ. Saf.*, 2021, **212**, 111969.
9 Y. Sun, J. Liang, L. Tang, H. Li, Y. Zhu, D. N. Jiang, B. Song, M. Chen and G. M. Zeng, *Nano Today*, 2019, **28**, 100757.
10 S. J. Song, Y. L. Wang, J. Xie, B. H. Sun, N. L. Zhou, H. Shen and J. Shen, *ACS Appl. Mater. Interfaces*, 2019, **11**, 34258–34267.
11 S. E. El-Abeid, Y. Ahmed, J. A. Daròs and M. A. Mohamed, *Nanomaterials*, 2020, **10**, 1001.
12 H. X. Zhu, Y. Shen, J. X. Cui, A. Q. Wang, N. J. Li, C. Wang, B. Cui, C. J. Sun, X. Zhao, C. X. Wang, F. Gao, S. S. Zhan, L. Guo, L. Zhang, Z. H. Zeng, Y. Wang and H. X. Cui, *Ind. Crops Prod.*, 2020, **152**, 11249.
13 S. J. Song, H. Shen, Y. L. Wang, X. H. Chu, J. Xie, N. L. Zhou and J. Shen, *Colloids Surf., B*, 2020, **185**, 110596.
14 A. Rawal, S. H. C. Man, V. Agarwal, Y. Yao, S. C. Thickett and P. B. Zetterlund, *ACS Appl. Mater. Interfaces*, 2021, **13**, 18255–18263.
15 M. A. Jihad, F. T. M. Noori, M. S. Jabir, S. Albukhaty, F. A. AlMalki and A. A. Alyamani, *Molecules*, 2021, **26**, 3067.

16 S. Pathmanapan, P. Periyathambi and S. K. A. Sadagopan, *Nanomedicine*, 2020, **29**, 102251.
17 X. J. Zhang, Q. M. Gao, Q. F. Zhuang, L. Zhang, S. H. Wang, L. B. Du, W. X. Yuan, C. F. Wang, Q. Tian, H. Yu, Y. M. Zhao and Y. Liu, *RSC Adv.*, 2021, **11**, 10986–10995.
18 Y. J. Tong, L. H. Shao, X. L. Li, J. Q. Lu, H. L. Sun, S. Xiang, Z. H. Zhang, Y. Wu and X. M. Wu, *J. Agric. Food Chem.*, 2018, **66**, 2616–2622.
19 Y. Wang, C. N. Li, T. Wang and X. G. Li, *Langmuir*, 2020, **36**, 12336–12345.
20 S. J. Song, M. H. Wan, W. L. Feng, J. Zhang, H. Mo, X. F. Jiang, H. Shen and J. Shen, *ACS Agric. Sci. Technol.*, 2021, **1**, 182–191.
21 M. S. Muda, A. Kamari, S. A. Bakar, S. N. M. Yusoff, I. Fatimah, E. Phillip and S. M. Din, *J. Mol. Liq.*, 2020, **318**, 114066.
22 X. P. Wang, H. C. Xie, Z. Y. Wang, K. L. He and D. P. Jing, *Environ. Sci.: Nano*, 2019, **6**, 75.
23 G. G. Rolim, R. R. Coelho, J. D. Antonino, L. S. Arruda, A. S. Rodrigues, E. M. Barros and J. B. Torres, *Pest Manage. Sci.*, 2021, **77**, 4400–4410.
24 W. B. Zhang, G. Tang, H. Q. Dong, Q. Q. Geng, J. F. Niu, J. Y. Tang, J. L. Yang, H. Huo and Y. S. Cao, *Colloids Surf., B*, 2019, **178**, 153–162.
25 Z. R. Akhtar, K. Tariq, A. M. Handler, A. Ali, F. Ullah, F. Ali, L. S. Zang, A. Gulzar and S. Ali, *Ecotoxicology*, 2021, **30**, 448–458.
26 J. C. Chen, Y. J. Gong, P. Shi, Z. H. Wang, L. J. Cao, P. Wang and S. J. Wei, *Exp. Appl. Acarol.*, 2019, **77**, 545–554.
27 J. W. S. Hummers and R. E. Offeman, *J. Am. Chem. Soc.*, 1958, **80**, 1339.
28 W. N. Wu, M. H. Wan, Q. Fei, Y. Tian, S. J. Song, H. Shen and J. Shen, *Pest Manage. Sci.*, 2021, **77**, 4960–4970.
29 S. S. Su, Y. H. Tian, Y. Y. Li, Y. P. Ding, T. J. Ji, M. Y. Wu, Y. Wu and G. J. Nie, *ACS Nano*, 2015, **9**, 1367–1378.
30 P. L. Ritger and N. A. Peppas, *J. Controlled Release*, 1987, **5**, 23–36.
31 F. Campos, D. A. Krupa and R. Jansson, *J. Econ. Entomol.*, 1997, **90**, 742–746.
32 K. H. Kabir and R. B. Chapman, *J. Econ. Entomol.*, 1997, **90**, 272–277.
33 Y. B. Sun, Y. Chen, T. Liu, Y. Y. Wang, Y. Wang, L. R. Han, Z. Q. Ma and J. T. Feng, *J. Plant Dis. Prot.*, 2021, **128**, 1263–1268.
34 S. Y. Wu, H. C. Xie, M. Y. Li, X. N. Xu and Z. R. Lei, *Exp. Appl. Acarol.*, 2016, **70**, 421–435.
35 W. S. Abbott, *J. Econ. Entomol.*, 1925, **18**, 265–267.
36 M. Ahmad and R. M. Hollingworth, *Pest Manage. Sci.*, 2004, **60**, 465–473.
37 E. S. Ganya, S. J. Moloi, S. C. Ray and W. F. Pong, *J. Mater. Res.*, 2020, **35**, 2478–2490.
38 M. A. Kamal, S. Bibi, S. W. Bokhari, A. H. Siddique and T. Yasin, *React. Funct. Polym.*, 2017, **110**, 21–29.
39 X. Jing, H. Y. Mi, B. N. Napiwocki, X. F. Peng and L. S. Turng, *Carbon*, 2017, **125**, 557–570.
40 F. Cataldo, *Fullerenes, Nanotubes, Carbon Nanostruct.*, 2003, **11**, 1–13.
41 H. Qin, H. Zhang, L. X. Li, X. T. Zhou, J. P. Li and C. Y. Kan, *RSC Adv.*, 2017, **7**, 52684–52693.
42 S. J. Song, X. F. Jiang, H. Shen, W. N. Wu, Q. Q. Shi, M. H. Wan, J. Zhang, H. Mo and J. Shen, *ACS Appl. Bio Mater.*, 2021, **4**, 6912–6923.
43 S. Liu, T. H. Zeng, M. Hofmann, E. Burcombe, J. Wei, R. Jiang, J. Kong and Y. Chen, *ACS Nano*, 2011, **5**, 6971–6980.
44 M. Ahmad and R. M. Hollingworth, *Pest Manage. Sci.*, 2004, **60**, 465–473.
45 Y. H. Gao, Y. N. Xiao, K. K. Mao, X. Y. Qin, Y. Zhang, D. L. Li, Y. H. Zhang, J. H. Li, H. Wan and S. He, *Chem. Eng. J.*, 2020, **383**, 123169.
46 S. H. Li, A. J. Stein, A. Kruger and R. M. Leblanc, *J. Phys. Chem. C*, 2013, **117**, 16150–16158.
47 W. Z. Cai, X. F. Pang, B. Z. Hua, G. W. Liang and D. L. Song, *General Entomology*, China Agricultural University Press, Beijing, 2011, p. 101.
48 R. Jettera and R. Sodhib, *Surf. Interface Anal.*, 2011, **43**, 326–330.
49 S. Sharma, B. Singh, P. Bindra, P. Panneerselvam, N. Dwivedi, A. Senapati, A. Adholeya and V. Shanmugam, *ACS Appl. Mater. Interfaces*, 2021, **13**, 9143–9155.
50 J. Shang, Y. N. Guo, D. L. He, W. Qu, Y. N. Tang, L. Zhou and R. L. Zhu, *J. Hazard. Mater.*, 2021, **416**, 125706.